



Contents lists available at ScienceDirect



Catalysis Today

journal homepage: www.elsevier.com/locate/cattod

Syntheses, characterization and catalytic activities of CaAl-layered double hydroxide intercalated Fe(III)-amino acid complexes

Gábor Varga^{a,b}, Zita Timár^{a,b}, Szabolcs Muráth^{a,b}, Zoltán Kónya^{c,d}, Ákos Kukovecz^{c,e}, Stefan Carlson^f, Pál Sipos^{b,g}, István Pálkinkó^{a,b,*}

^a Department of Organic Chemistry, University of Szeged, Dóm tér 8, Szeged, H-6720 Hungary

^b Materials and Solution Structure Research Group, Institute of Chemistry, University of Szeged, Aradi Vértanúk tere 1, Szeged, H-6720 Hungary

^c Department of Applied and Environmental Chemistry, University of Szeged, Rerrich Béla tér 1, Szeged, H-6720 Hungary

^d MTA-SZTE Reaction Kinetics and Surface Chemistry Research Group, Rerrich Béla tér 1, Szeged, H-6720 Hungary

^e MTA-SZTE "Lendület" Porous Nanocomposites Research Group, Rerrich Béla tér 1, Szeged, H-6720 Hungary

^f Max-IV Laboratory, Lund University, Lund, Sweden

^g Department of Inorganic and Analytical Chemistry, University of Szeged, Dóm tér 7, Szeged, H-6720 Hungary

ARTICLE INFO

Article history:

Received 26 August 2016

Received in revised form 10 October 2016

Accepted 1 December 2016

Available online xxxx

Keywords:

Structural characterisation

Fe(III)-amino acid complexes in CaAl-LDH

Catalytic properties

Oxidation reactions

Ullman-type etherification

ABSTRACT

Synthesis of intercalated composites were carried out using CaAl-LDH (layered double hydroxide) as host and the anionic form of Fe(III)-amino acid complexes as guest materials. Intercalation was attempted with two methods either introducing the preformed complexes or constructing the complex among the layers of the LDH. After optimization of the synthesis parameters, structural characterization was performed by X-ray diffractometry, scanning electron microscopy as well as mid and far infrared spectroscopies. Quantitative data about the intercalated complexes were collected by chemical analysis and X-ray absorption spectroscopy investigating the near edge region as well as the extended fine structure. Structural models based on characterization measurements are also given. Catalytic activities, selectivities and recycling abilities of the substances were studied in the oxidation reactions of cyclohexene with peracetic acid and *in situ* formed iodosylbenzene as oxidants in the liquid phase. The catalysts were active in the Ullmann-type etherification coupling reaction as well. The intercalated substances were found to be efficient and highly selective catalysts with very good recycling abilities.

© 2016 Elsevier B.V. All rights reserved.

1. Introduction

Homogeneous catalysts are most often complex compounds containing a metal (ion) and various organic compounds as ligands [1]. They can be highly active and extremely selective. However, their recovery from the reaction mixture and, therefore, their reuse is usually difficult if not impossible. Heterogenisation is a common method of eliminating these drawbacks [2,3], although some activity and selectivity losses may be expected. A chance of minimizing these disadvantageous features may be offered if immobilization occurs by keeping the identity of the complex. Moreover, if immobilization is performed in a constrained environment [4], e.g., among the layers of layered double hydroxides (LDHs) [5–7], the shape selective effects of the host material may be exploited.

Fe(III)-containing amino acid complexes, as the cofactors in various oxidoreductase enzymes are found in nature as the redox centres of these biological catalysts. As redox catalysts, they have important role in laboratory organic transformations as well. In order to facilitate easier recovery and increase durability, these complexes are frequently anchored to various host materials like functionalized silica gel [8] or zeolite [9]. However, to the best of our knowledge such compounds have never been introduced among the layers of LDHs of any type.

LDHs, because of the relative ease of their synthesis, represent inexpensive, versatile and potentially recyclable source of catalyst supports [10–12], catalyst precursors [13–15] or actual catalysts [16–19]. LDHs can be found in nature, but for applications they are usually synthesized. They have many representatives, and they have been classified [20]. Part of the hydrotalcite supergroup is the hydrocalumite subgroup – the name giving mineral has the formula of $[Ca_2Al(OH)_6]A \times nH_2O$, where A is a monovalent anion – having corrugated brucite-like main layers, which contain ordered arrangements of Ca^{2+} and Al^{3+} or other trivalent ions, seven- and

* Corresponding author at: Department of Organic Chemistry, University of Szeged, Dóm tér 8, Szeged, H-6720 Hungary.

E-mail address: palinko@chem.u-szeged.hu (I. Pálkinkó).

six-coordinated, respectively, in a fixed molar ratio of 2:1. The layers are positively charged, which is compensated by interlayer anions. The anions are exchangeable with more or less difficulties, and even bulkier anions can be introduced into the interlayer space. In the experimental work leading to this contribution, hydrocalumite, CaAl-LDH in the followings, was chosen as the host material.

A lot of methods of LDH synthesis have been elaborated [21,22]; nevertheless, the synthesis of LDHs is most often performed by a wet chemical method. It is called co-precipitation, when the LDH is produced from the mixed solution of salt components by a base solution. An LDH is an intercalated system even as-prepared due to the charge-balancing anions among the layers. These ions can be exchanged with various methods. In this work, varieties of direct anion exchange were applied. The guests were Fe(III)-amino acid (*L*-cysteine, *L*-histidine and *L*-tyrosine) complex anions. Synthesis methods were optimized to arrive at composites having the complex exclusively among the layers. The comprehensively characterized organic-inorganic composites were used as catalysts in various oxidation reactions.

Metal complexes have already been incorporated in LDHs, and the early works have been reviewed [23]. Complexes of various transition metal ions (Ni(II), Co(II), Fe(II), Ir(III), Mo(IV, VI), Ru(II), ReO₂(V)) have been intercalated; however, Fe(III) was only incorporated as Fe(CN)₆³⁻ complex anion. Since then, we could only identify only three paper published recently [24–26]. In two of them, Fe(III)-porphyrin derivatives were intercalated in ZnAl- [24] and MgAl-LDHs [25], and the obtained materials were used in the oxidation of cyclooctene, cylohexene, cyclohexane and over the latter composite even heptane applying iodosylbenzene as oxidant. In a very recent article, four sulphonato-Schiff bases were used as ligands [26]. The catalytic properties of these intercalated complexes were tested in the selective oxidation of glycerol to glyceric acid. The Fe(III)-containing composites were active catalysts, but the Cu(II)-containing ones had superior performance.

In this contribution, the results of our experimental work concerning the syntheses, the structural characterization and the catalytic activities of novel Fe(III)-amino acid complex anion containing CaAl-LDHs are communicated.

2. Experimental part

2.1. Materials and the methods of synthesis

The LDH host containing nitrate as charge-compensating anions among the layers was prepared by the co-precipitation method. A mixture of Ca(NO₃)₂·4H₂O (30 mmol) and Al(NO₃)₃·9H₂O (15 mmol) was dissolved in 100 ml of distilled water, and was stirred at pH 13 for 12 h. The suspension was filtered and dried for 24 h.

For constructing the Fe(III)-amino acid anions among the layers, two methods were used adopted from those applied for the syntheses of Mn(II)-amino acid anion–CaAl-LDH and Cu(II)-amino acid–CaAl-LDH composites [27,28]. In brief, the preparation method consisted of the following steps.

In *Method 1*, the amino acid anions were intercalated first, and it was followed by the introduction of the Fe³⁺ ions. In the first step, 2.5×10⁻³ moles of *L*-cysteine, *L*-histidine or *L*-tyrosine were used for the intercalation. The iron ions were introduced in the solution in various amounts (the molar ratio of the amino acid and the iron ions varied from 1:2 to 1:8). In order to identify the optimum conditions, the solvents (aqueous ethanol, aqueous acetone or water) and the pH (from 7.5 to 9.5) were also varied. Designation of composites prepared with *Method 1* is going to be CaAl–Fe(III)-amino acid anion–LDH in the followings.

In *Method 2*, the Fe(III)-amino acid complexes were prepared separately applying the same amounts and ratios as well as varying the solution and the pH in the same way as in *Method 1*. Then, the solution containing the complex anion was used for the intercalation. From now on, designation of the composites prepared with *Method 2* is going to be Fe(III)-amino acid anion–CaAl-LDH.

All synthetic operations were performed under N₂ protecting gas to exclude airborne CO₂ reacting with the water content of the LDH forming carbonate ion, which readily intercalates inhibiting the introduction of any other anion.

All the applied compounds are the products of analytical grade from Sigma-Aldrich, and they were used as received.

2.2. Methods of structural characterization

X-ray diffraction (XRD) patterns were recorded on a Rigaku XRD-6000 diffractometer using CuK α radiation ($\lambda = 0.15418 \text{ nm}$) at 40 kV, 30 mA. The UV-vis spectra were collected on a Shimadzu UV-1650 spectrophotometer. The morphologies of the various composite samples were investigated using a scanning electron microscope (SEM Hitachi S-4700) with the accelerating voltage of 10–18 kV. Energy dispersive X-ray (EDX) analysis data are obtained with a Röntec QX2 energy dispersive microanalytical system from two different parts of the sample. The coupled system also provides with the elemental map.

The amount of metal ions between the layers was measured on a Thermo's IRIS Intrepid II ICP-OES spectrometer. Before measurements, a few milligrams of the intercalated complexes measured by analytical accuracy were digested in 1 cm³ cc. H₂SO₄; then, they were diluted with distilled water to 50 cm³ and filtered. The reaction mixtures, after filtering the used catalysts, were also analyzed for possible leached out metal ions.

X-ray absorption spectroscopic (XAS) measurements were carried out at the K-edge of the manganese at MAX-lab at beamline I811. This is a superconducting multipole wiggler beamline equipped with a water-cooled channel cut Si(111) double crystal monochromator delivering at 10 keV, approximately 2 × 10¹⁵ photons/s/0.1% bandwidth with horizontal and vertical FWHM of 7 and 0.3 mrad, respectively. A beam-size of 0.5 mm × 1.0 mm (width × height) was used. The incident beam intensity (I₀) was measured with an ionization chamber filled with a mixture of He/N₂. Higher order harmonics were reduced by detuning the second monochromator to 70% of the maximum intensity. Data collection was performed in the fluorescent mode. The samples were contained in Teflon spacers with Kapton tape windows. Their amounts were adjusted to the iron concentration. Data were treated with EXAFSPAK software package [29].

Three different IR (infrared) techniques were combined in order to distinguish organic moieties bound to the outer surface from those located among the layers. The photoacoustic detection is sensitive to the bulk of the composites (scan speed 2500 Hz), while ATR (attenuated total reflectance) mode detection collects information overwhelmingly from the outer surface of the samples. The diffuse reflectance mode unifies both previous detection forms, *i.e.*, surface and bulk information together become simultaneously available. The spectra were recorded with a BIO-RAD Digilab Division FTS-65A/896 FT-IR (Fourier-transform infrared) spectrophotometer with 4 cm⁻¹ resolution. The 4000–600 cm⁻¹ wavenumber range was investigated. 256 scans were collected for each spectrum.

Metal (ion)-ligand vibrations are directly seen in the far IR spectra recorded on a BIO-RAD Digilab Division FTS-40 vacuum FT-IR spectrophotometer with 4 cm⁻¹ resolution. Here, too, 256 scans were collected for each spectrum. The Nujol mull technique was

used between two polyethylene windows (the suspension of 10 mg sample and a drop of Nujol mull).

2.3. Catalytic measurements

The composites as catalysts were tested in the oxidative transformations of cyclohexene in the liquid phase. The parameters of the reaction were altered in order to find the optimal conditions. The reaction time (1–24 h), the amount of catalyst (10–75 mg), the reaction temperature (288–328 K), the solvents (acetone, dichloromethane and ethanol) as well as the oxidants (peracetic acid, (diacetoxyiodo)benzene) were varied. Optimum reaction conditions were identified as follows: 50 mg of catalyst, 10 cm³ of solvent (acetone when peracetic acid or aqueous acetone (5% water, 95% acetone by volume) when (diacetoxyiodo)benzene was used), 5 mmol of cyclohexene, 2.5 mmol of peracetic acid and 313 K or (diacetoxyiodo)benzene and 323 K with 6 h reaction time.

Furthermore, the composites were tested in the Ullmann diaryl etherification reaction [30]. As auxiliary materials, pyridine, piperidine and inorganic bases were applied. Toluene, dimethyl formamide (DMF) or ethanol were tried as solvents, the amount of the catalyst and the temperature of the reaction were varied in the 25–100 mg and 298–383 K ranges, respectively. Optimum reaction conditions were identified as follows: 75 mg of catalyst, 5 cm³ of toluene (when inorganic base is used, it is dissolved in 0.5 cm³ of water), 0.6 mmol of iodobenzene, 0.5 mmol of phenol, 0.5 mmol of base, 24 h reaction time at 368 K.

At the end of the reactions, the mixtures were analysed on a Hewlett-Packard 5890 Series II gas chromatograph equipped with flame ionization detector, using an Agilent HP-1 column and the internal standard technique using toluene. The temperature was increased in stages from 50 °C to 250 °C. The products were identified via using authentic samples.

Conversions as well as turnover frequency (TOF) data are given and were calculated from data obtained at the end of the reaction. The former is defined as the (mol) percentage of the reactant consumed and the latter as the number of molecules reacted at one Fe(III) ion in 1 h.

3. Results and discussion

3.1. Characterization of the composite LDHs

The aims of the synthetic work were to identify those composites where the intercalation was successful, and the complexes resided preferably among the layers. The first is the priority goal, but the second one is also important. Probably, Fe(III)-amino acid complexes adsorbed on the outer surface of the host material exhibit catalytic activities; however, they are prone to leaching to a much higher degree than those incorporated among the layers.

The major experimental tools for selecting these samples were X-ray diffractometry and IR spectroscopy with two detection modes (PA-IR and ATR-IR).

If the characteristic reflections in the X-ray diffractograms of the composites are shifted to lower 2θ values relative to the as-prepared pristine (containing only simple inorganic anions) LDH, the success of intercalation can confidently be stated.

In Fig. 1, the X-ray diffractograms of those samples and that of the pristine LDH (for comparison) are depicted where shifts, like mentioned above, were seen. They were observed for the Fe(III)-histidinate- and Fe(III)-tyrosinate-containing composites prepared by Method 1 and Fe(III)-cysteinate-containing one made by Method 2. The reflections of the intercalated LDH is only seen for the Fe(III)-cysteinate containing sample (the shift in the positions of the most easily observable first two reflections toward lower angles is mod-

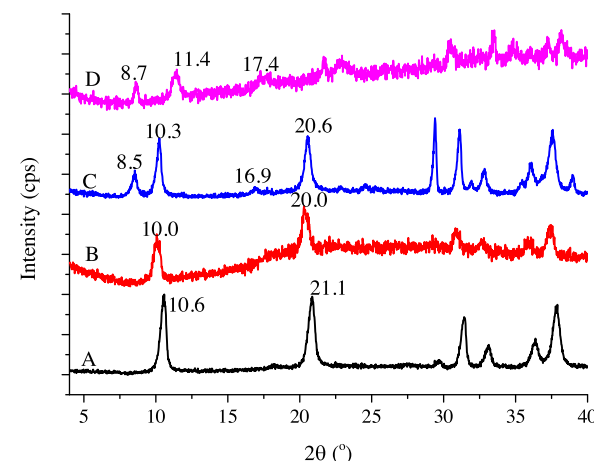


Fig. 1. X-ray diffractograms of A: CaAl-LDH; B: CaAl-Fe(III)-cysteinate-LDH; C: Fe(III)-histidinate-CaAl-LDH; D: Fe(III)-tyrosinate-CaAl-LDH (optimal parameters: 1:4 = Fe(III):amino acid (nominal); aqueous ethanol solvent).

Table 1

Basal spacing and interlayer distance values for the pristine and the intercalated materials (the thickness of one layer is 0.234 nm [32]).

Substances	Basal spacing (<i>d</i>) (nm)	Interlayer distance (nm)
CaAl-LDH	0.857	0.623
CaAl-Fe(III)-cysteinate-LDH	0.883	0.649
Fe(III)-histidinate-CaAl-LDH	1.039	0.805
Fe(III)-tyrosinate-CaAl-LDH	1.014	0.780

erate but clear). The shifts for the other two samples are more pronounced; however, intercalation proceeded in steps (it is called staging [31]), beside the reflections of the composite those of the pristine LDH are also seen.

The basal spacings calculated from the first reflections of the X-ray traces are summarized in Table 1.

A comparison of the ATR- and PA-IR spectra reveals that the Fe(III)-tyrosinate- and Fe(III)-cysteinate-bearing composites contain the complexes (in their anionic form) only in their interlayer spaces (Fig. 2). It is proven by the appearance of new vibrations in the PA-IR spectra (~ 1140 and ~ 1240 cm⁻¹) and the shifted carboxylate group vibrations (~ 1620 and 1640 cm⁻¹). Unfortunately, this cannot be claimed about the Fe(III)-histidinate-containing sample. Even though shifted carboxylate vibrations are seen, but the ATR-IR spectrum consists of vibrations not seen on that of the pristine LDH.

The composition as well as the metal ion to ligand ratios in the intercalated complexes were measured by UV-vis spectroscopy and ICP-OES analysis. Data are summarized in Table 2. It is to be seen that all the samples contained Fe(III) ions, and the actual metal ion to ligand ratios were all close to 1:2. It indicates that the amount amino acid ions not involved in complexation is negligible.

3.2. Characterization of the intercalant

3.2.1. XAS measurements

The Fe K-edge X-ray absorption spectra, detected all for composites, are displayed in Fig. 3.

The X-ray absorption spectrum of the sample (Fig. 3) near the absorption edge, shows a very weak pre-edge peak at 7130 eV corresponding to $1s \rightarrow 3d$ transition in the Fe³⁺ ion. For a centrosymmetric octahedral site, the only intensity mechanism available for the allowed $1s \rightarrow 3d$ feature is the allowed electric quadrupole transition. An octahedral high-spin ferric complex should show two pre-edge features; however, it can only be

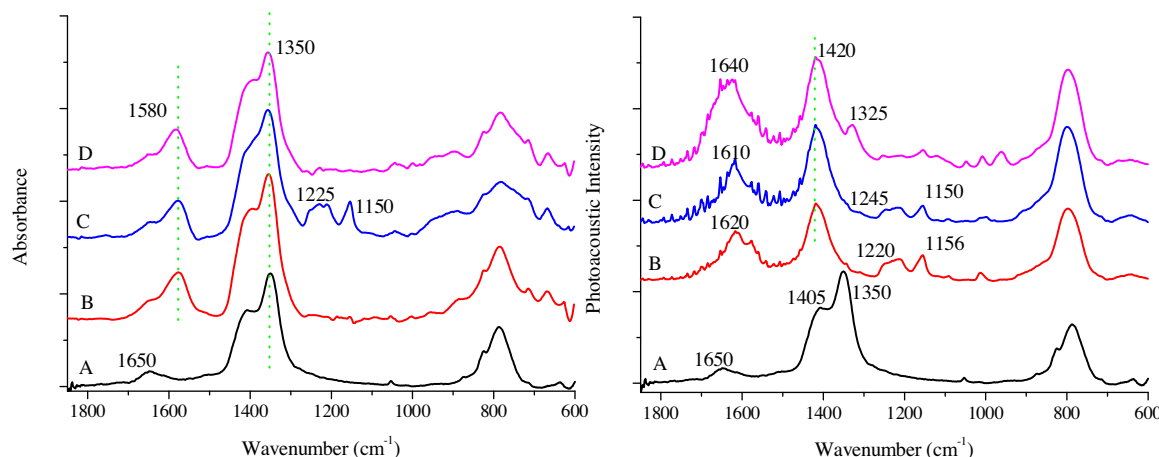


Fig. 2. ATR-IR (left) and PA-IR (right) spectra of A: CaAl-LDH; B: CaAl-Fe(III)-cysteinate-LDH; C: Fe(III)-histidinate-CaAl-LDH; D: Fe(III)-tyrosinate-CaAl-LDH.

Table 2

Quantitative analytical data of the intercalant in the selected composites.

Composites	Amino acid (mol/0.3 g LDH)	Fe(III) (mol/0.3 g LDH)	Amino acid/Fe(III)
CaAl-Fe(III)-cysteinate-LDH	8.0×10^{-4}	3.7×10^{-4}	2.16
Fe(III)-histidinate-CaAl-LDH	2.5×10^{-4}	1.3×10^{-4}	1.92
Fe(III)-tyrosinate-CaAl-LDH	6.9×10^{-4}	3.3×10^{-4}	2.09

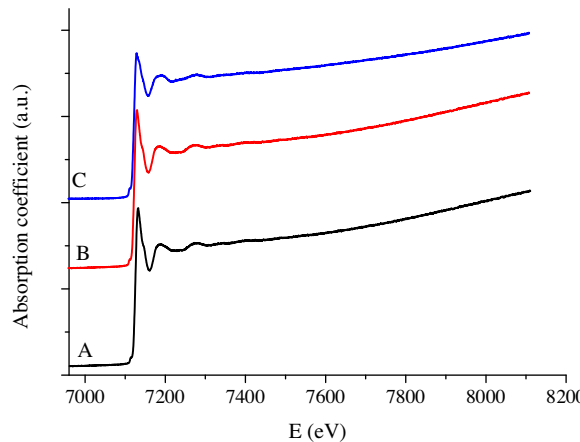


Fig. 3. Fe-K-edge X-ray absorption spectra of A: CaAl-Fe(III)-cysteinate-LDH; B: Fe(III)-histidinate-CaAl-LDH; C: Fe(III)-tyrosinate-CaAl-LDH.

detected with high-resolution XAS [33]. These results mean that octahedral geometry can be suggested in all cases.

The EXAFS (extended X-ray absorption fine structure) data were k^3 -weighted and Fourier transformed in the range of $k = 2\text{--}9 \text{\AA}^{-1}$ (Fig. 4). The ranges for the backtransform were 1–4.5 Å for all complexes. The fitted parameters included interatomic distances (R), Debye–Waller factors (σ^2). The coordination numbers (N) were kept constant during each optimisation, but a range of coordination numbers were used to find the best fit. The k^3 -weighted EXAFS spectra are shown in Fig. 4, and the results of the fitting are reported in Table 3.

Data in Table 3 indicate octahedral geometry for each composite. Two different interatomic distances could be determined for the Fe(III)-tyrosinate-, and Fe(III)-histidinate-containing composites. They belong to Fe–O/N distances. Unfortunately, by these measurements the difference between oxygen and nitrogen cannot be estimated clearly, since O and N atoms scatter the photoelectrons nearly the same way, since their atomic masses are very close to each other. For the Fe(III)-cysteinate-containing composite, the

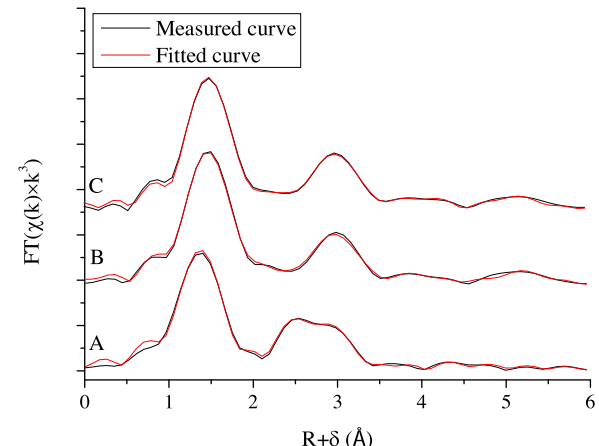


Fig. 4. Observed and fitted Fe(III)-K-edge radial distribution functions of A: CaAl-Fe(III)-cysteinate-LDH; B: Fe(III)-histidinate-CaAl-LDH; C: Fe(III)-tyrosinate-CaAl-LDH.

best fit indicates that sulphur is involved in the first coordination sphere.

3.2.2. Far IR measurements

Fe(III)-coordinating atom interaction can be directly detected in the far IR region. The identification of vibrations was done with the help of the correlations published recently [34]. The spectra of the pristine LDH and those of the composites are seen in Fig. 5. The vibration observed near 392 cm^{-1} is attributed to Fe(III)–O_{carboxylate} interaction in the spectra of CaAl–Fe-cysteinate–LDH and Fe-histidine–CaAl–LDH. The spectrum of the Fe-tyrosinate–CaAl–LDH composite contains a band at 267 cm^{-1} , which can be attributed to Fe(III)–amino nitrogen vibration. The band at 220 cm^{-1} , in the spectrum of Fe-histidine–CaAl–LDH is assigned to Fe(III)–N_{imidazolate} pair interaction.

Table 3

Parameters calculated from the fitted EXAFS spectra (N: coordination number, R: bond length, σ^2 Debye-Waller factor, F-factor: goodness of fit).

CaAl-LDH sample	Fe(III)-X	N	R(Å)	σ^2 (\AA^2)	R factor
Fe(III)-tyrosinate	N/O	4	2.00	0.0091	0.105
	N/O	2	2.18	0.014	
Fe(III)-cysteinate	N/O	2	1.98	0.0043	0.145
	N/O	2	2.17	0.0071	
	S	2	2.36	0.0091	
Fe(III)-histidinate	N/O	4	1.96	0.0035	0.106
	N/O	2	2.16	0.0099	

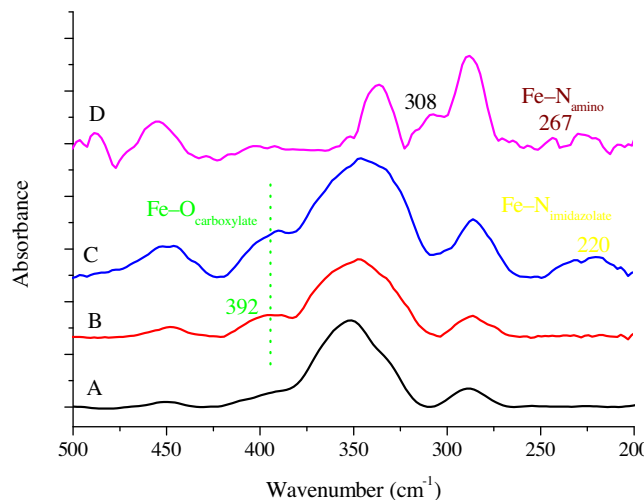


Fig. 5. Far IR spectra of A: CaAl-LDH; B: CaAl-Fe(III)-cysteinate-LDH; C: Fe(III)-histidinate-CaAl-LDH; D: Fe(III)-tyrosinate-CaAl-LDH.

3.3. SEM images and elemental maps of the composites

Visualization of the morphologies of the composites becomes possible by using SEM measurement. The selected intercalated sub-

stances all display the laminar, hexagonally-shaped morphology typical of LDHs (Fig. 6).

The elemental map constructed from EDX measurements provides with additional proof that sulphur is present in the CaAl-Fe(III)-cysteinate-LDH composite, and it seems to be evenly distributed (Fig. 7).

3.4. Models of the intercalated iron-amino acid complexes

Unifying the various pieces of information obtained by analytical and structural characterization methods complementing with chemical common sense, the following picture emerges for the intercalated complexes.

The Fe(III) ions in the intercalated complexes are octahedrally coordinated (XAS), and the ligands coordinate in a multidentate, most probably, bidentate manner (chemical analysis). Higher degree of coordination is not possible because of steric reasons, and, therefore, the remaining two coordination sites have to be filled with water molecules (XAS). Water molecules are integral parts of an LDH structure; they are abundant among the layers, therefore, they are readily available for coordination. The major coordinating atoms in the composites are the carboxylate oxygen (CaAl-Fe-cysteinate-LDH and Fe-histidinate-CaAl-LDH – XAS, far IR), the imidazole nitrogen (Fe-histidinate-CaAl-LDH – XAS, far IR),

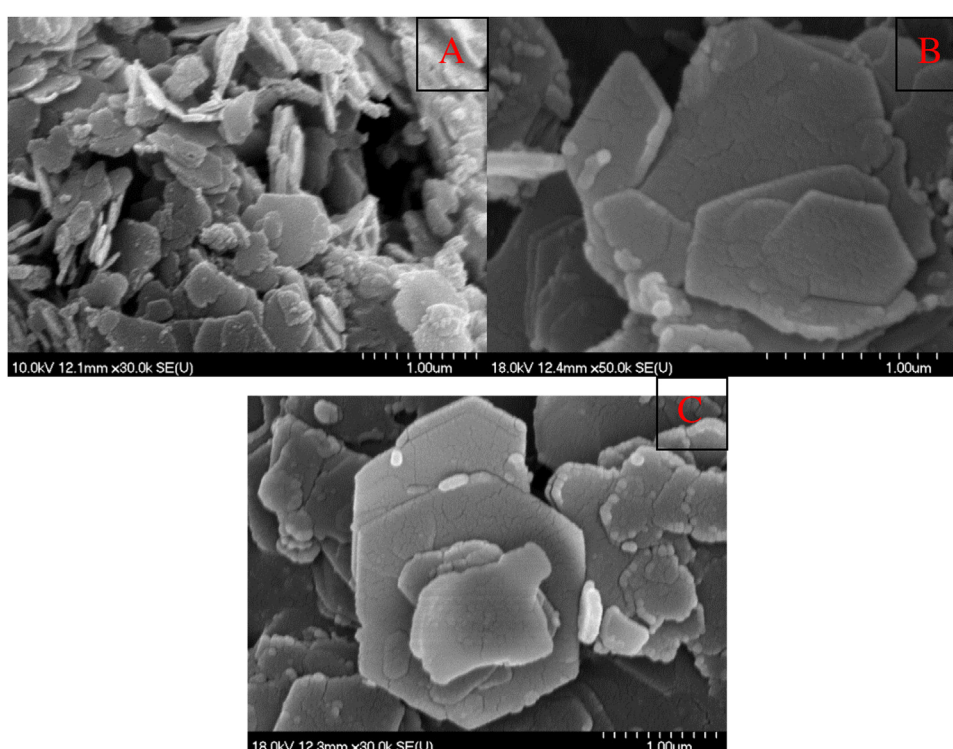


Fig. 6. A: CaAl-Fe(III)-cysteinate-LDH; B: Fe(III)-histidinate-CaAl-LDH; C: Fe(III)-tyrosinate-CaAl-LDH.

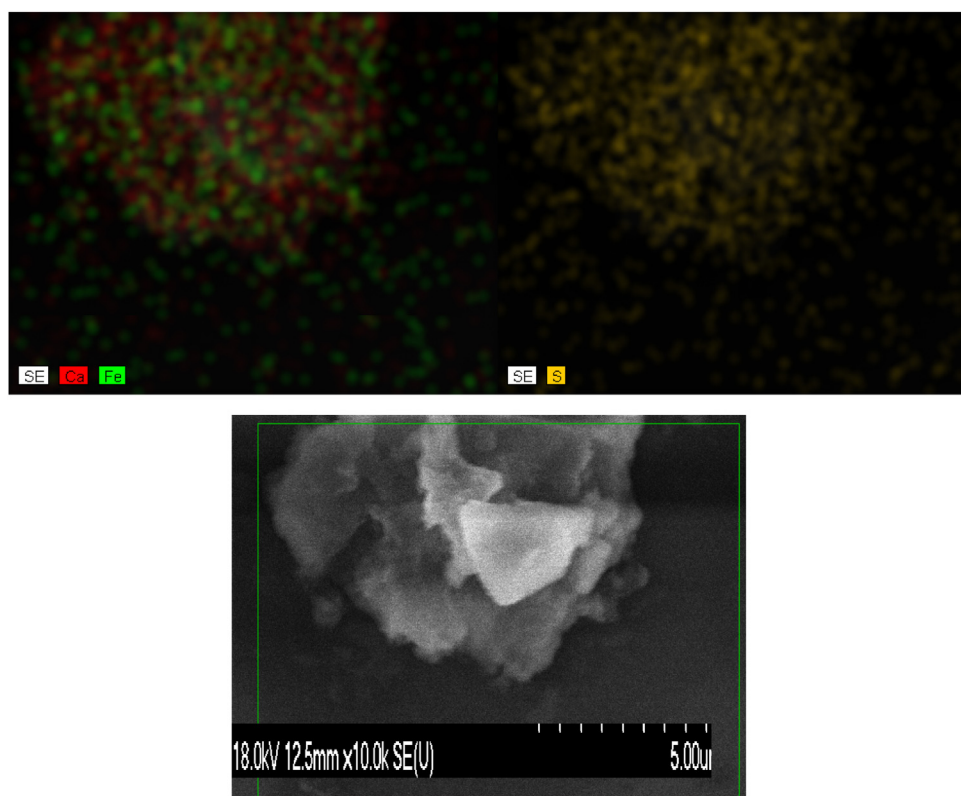


Fig. 7. The SEM–EDX elemental map of the CaAl–Fe(III)–cysteinate–LDH sample.

Table 4

The TOF/conversion and selectivity results of the oxidation of cyclohexene after 6 h (catalyst: 50 mg, acetone: 10 cm³, cyclohexene: 5 mmol, peracetic acid: 2.5 mmol, temperature: 313 K).

Composites	TOF (1/h)/conversion (%)	Epoxide (%)	2-Chex-1-ol (%)	2-Chex-1-one (%)	trans Diol (%)
—	nr/18	67	10	1	22
CaAl-LDH	nr/18	66	10	2	22
Fe(III)-tyrosinate-CaAl-LDH	61/45	88	—	—	12
CaAl–Fe(III)–cysteinate–LDH	77/51	94	3	1	2
Fe(III)-histidinate-CaAl-LDH	169/44	100	—	—	—

the nitrogen atom of the amino group (Fe-tyrosinate–CaAl-LDH – XAS, far IR) and sulphur atom of the thiolate group (CaAl–Fe-cysteinate–LDH – XAS). In the Fe-tyrosinate–CaAl-LDH composite, the phenolate ions keep the complex among the layers of the LDH. The amino nitrogens and the phenolate oxygens cannot coordinate at the same time because of steric reasons (chemical common sense).

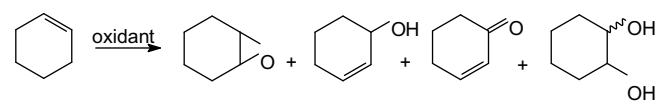
On the basis of the above-reasoning, using the data obtained from X-ray absorption measurements and knowing that the thickness of the layer is 0.234 nm [32] and the interlayer distances from XRD measurements, approximate models can be constructed for the composites, mainly to help visualisation (Fig. 8).

3.5. Catalytic properties of the composites

3.5.1. Cyclohexene oxidation

First, the composites were used in the oxidative transformations of cyclohexene. Two different oxidants were applied in these reactions, and significant differences were experienced in the rate of the transformations and product distributions.

Peracetic acid is a known epoxidation agent reacting stoichiometrically; however, in the presence of transition metal catalysts, it can be more reactive and can epoxidize alkenes with higher con-



Scheme 1. The oxidative transformations of cyclohexene.

versions under mild conditions. Fe(III) can act as a Lewis acid and can coordinate the organic peracid turning it to a potent oxidant.

In order to be able to study the oxidative transformations of cyclohexene, the decomposition of peracetic acid needs to be avoided. Acetone was found to be a perfect solvent: peracetic acid did not decompose in this solvent. The conversion and selectivity results of the intercalated catalysts in the oxidation of cyclohexene (Scheme 1) with peracetic acid in acetone are reported in Table 4.

It is to be seen that in all cases, the conversion of catalyzed reaction is significantly higher than that of the stoichiometric. The selectivities, which are significantly higher for the catalyzed reaction than for the stoichiometric one, virtually do not depend on the identity of the amino acid ligand.

The mechanism of the reaction is suggested as follows: one of the coordinated water molecules is replaced by the peroxidic oxygen donor oxidant forming (hydro)peroxyo-metal species, then, the O–O bond is cleaved heterolytically to form high-valent metal-oxo species as an active intermediate, which is responsible for the

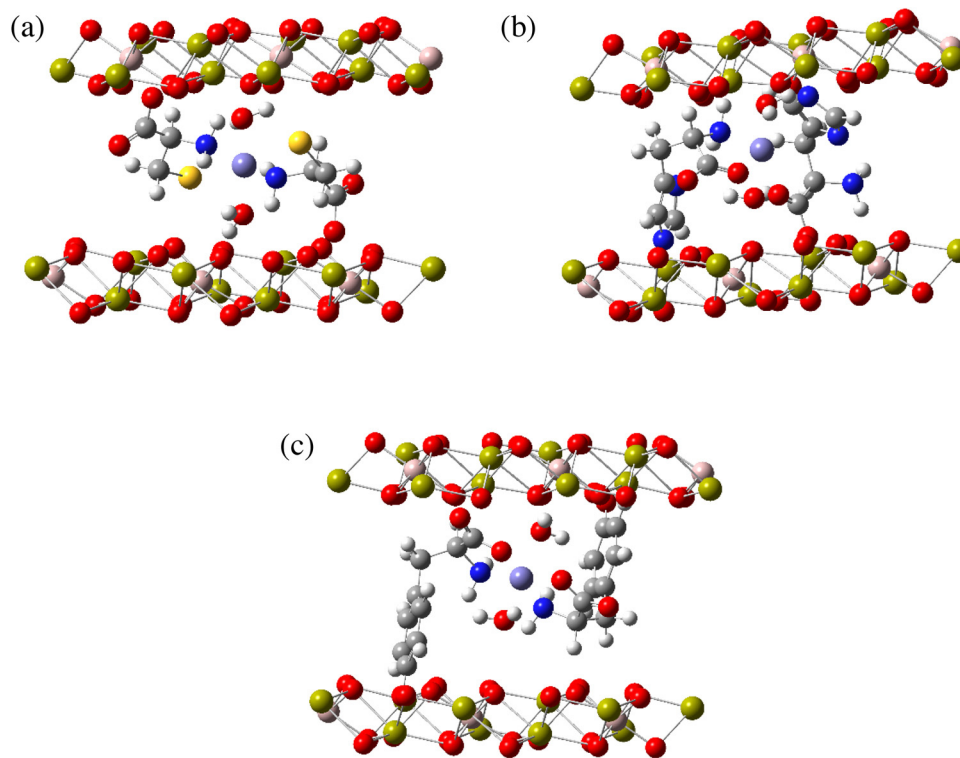


Fig. 8. The proposed steric arrangement of the intercalated complexes between the layers of CaAl-LDH based on XRD, XAS and far IR measurements, (a) CaAl-Fe(III)-cysteinate-LDH, (b) Fe(III)-histidinate-CaAl-LDH, (c) Fe(III)-tyrosinate-CaAl-LDH. The layer thickness is 0.234 nm [32] and the interlayer distances in the order of the models: 0.649 nm, 0.805 nm and 0.780 nm.

Table 5

Conversions in three rounds of recycling in the oxidation of cyclohexene after 6 h (catalyst: 50 mg, acetone: 10 cm³, cyclohexene: 5 mmol, peracetic acid: 2.5 mmol, temperature: 313 K, reactivation: rinsing with acetone).

Composites	Conv. 1. recycle (%)	Conv. 2. recycle (%)	Conv. 3. recycle (%)
Fe(III)-tyrosinate-CaAl-LDH	47	39	37
CaAl-Fe(III)-cysteinate-LDH	49	43	42
Fe(III)-histidinate-CaAl-LDH	44	46	40

Table 6

The TOF/conversion and selectivity results of the oxidation of cyclohexene after 6 h (catalyst: 65 mg, aqueous acetone (5/95% by volume): 10 cm³, cyclohexene: 5 mmol, (diacetoxido)benzene: 2.5 mmol, temperature: 323 K).

Composites	TOF (1/h)/conversion (%)	Epoxide (%)	2-Chex-1-ol (%)	2-Chex-1-one (%)	cis Diol (%)
—	nr/25	64	8	3	25
CaAl-LDH	nr/26	63	8	4	25
Fe(III)-tyrosinate-CaAl-LDH	43/41	17	—	—	83
CaAl-Fe(III)-cysteinate-LDH	63/54	—	—	—	100
Fe(III)-histidinate-CaAl-LDH	98/33	13	—	—	87

epoxidation of the uncoordinated cyclohexene. If both reactants are coordinated, there will be plenty of time for further reactions. If cyclohexene is coordinated alone, the situation will not be much different from the stoichiometric reaction. Thus, probably, the role of the ligands is to exert steric influence on the accessibility of the central ion by the reactants.

Acetic acid formed upon the decomposition peracetic acid was probably adsorbed over the outer surface of the LDH being of basic character; therefore, it could not initiate epoxide ring opening. This may be behind the very high epoxide selectivity.

The recycling abilities of the composites are also noteworthy; only slight deactivation is experienced even in the fourth run (Table 5). No special reactivation is required between the runs; the catalysts are only rinsed with acetone.

The process becomes diol-selective when (diacetoxido)benzene is used as the precursor of the real oxidant. This

Table 7

Conversions in three rounds of recycling in the oxidation of cyclohexene after 6 h (catalyst: 65 mg, aqueous acetone (5/95% by volume): 10 cm³, cyclohexene: 5 mmol, (diacetoxido)benzene: 2.5 mmol, temperature: 323 K, reactivation: rinsing with acetone).

Composites	Conv. 1. recycle (%)	Conv. 2. recycle (%)	Conv. 3. recycle (%)
Fe(III)-tyrosinate-CaAl-LDH	39	42	35
CaAl-Fe(III)-cysteinate-LDH	45	43	43
Fe(III)-histidinate-CaAl-LDH	31	28	29

compound is hydrolysed *in situ*, in the solvent (aqueous acetone – 5/95% by volume) according to the following equation [35]:

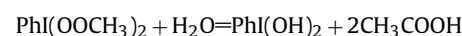


Table 8

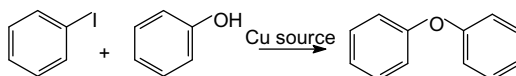
Conversion data of Ullmann reaction – the influence of the base (75 mg of catalyst, 5 cm³ of toluene (when inorganic base was used, it was dissolved in 0.5 cm³ of water), 0.6 mmol of iodobenzene, 0.5 mmol of phenol, 0.5 mmol of base, 24 h reaction time at 368 K).

Composites	Na ₂ CO ₃	K ₂ CO ₃	Pyridine	Piperidine
Fe(III)-tyrosinate-CaAl-LDH	19	20	53	45
CaAl-Fe(III)-cysteinate-LDH	21	24	40	36
Fe(III)-histidinate-CaAl-LDH	18	25	44	41

Table 9

Conversions in three rounds of recycling in the Ullmann reaction after 24 h (catalyst: 75 mg, toluene: 5 cm³, iodobenzene: 0.6 mmol, phenol: 0.5 mmol, pyridine: 0.5 mmol, temperature: 368 K, reactivation: rinsing with toluene).

Composites	Conv. 1. recycle (%)	Conv. 2. recycle (%)	Conv. 3. recycle (%)
Fe(III)-tyrosinate-CaAl-LDH	49	42	45
CaAl-Fe(III)-cysteinate-LDH	45	43	43
Fe(III)-histidinate-CaAl-LDH	41	38	39



Scheme 2. The Ullmann diaryl etherification (originally catalysed by copper species [30,36]).

The TOF/conversion and selectivity values obtained with the *in situ* generated PhI(OH)₂ are displayed in Table 6.

Data reveal that the *in situ* formed PhI(OH)₂ in the presence of added intercalated complexes produced almost exclusively the diol, even though epoxide is formed in appreciable quantities without them. The added composites act as catalysts, they largely retain their activities (Table 7) even in the third recycling experiments, and again they are only rinsed with the solvent after each run as the regeneration step. During recycling, only the *cis* diol is formed in the presence of each catalyst.

The *cis* diol, in the second reaction, could not be formed via epoxide intermediate. Rather, the transfer of the two OH groups could have occurred in a concerted manner *via* a cyclic intermediate. This way, the *cis* configuration could be assured.

3.5.2. The Ullmann-type diaryl etherification as test reaction

The composites actively catalysed the Ullmann-type etherification (Scheme 2), too. It is to be noted that there is no reaction without the LDH samples, and negligible activity is observed in the presence of the pristine LDH. Measured data are found in Table 8. In this reaction, the presence of the added base is important, and pyridine is proved to be the most efficient one.

The composites displayed very good recycling abilities (Table 9). The conversions remained high even after the third recycling reaction. For regeneration, a simple rinse with toluene proved to be sufficient.

The Ullmann diaryl etherification is a reaction known for a long time [30]. It has been conducted under either homogeneous or heterogeneous conditions, and much information has been collected. Originally, it was elaborated for copper species, and the vast majority of works still report results obtained in the presence of copper species (for a relatively recent review, see ref. [36]). It was problematic to use other transition metal species. Finally, it was found that FeCl₃ worked well [37]; however, high temperature (408 K) and long reaction time (20 h) was needed for high conversion (85%) in dimethyl formamide (DMF), and the catalyst was not recoverable. In toluene, the conversion was only 17% under the same conditions. Our composites performed significantly better in toluene at lower temperature, and they were recoverable. DMF cannot be applied with LDH-containing systems, because it destroys the layered structure and thus, the composites.

Let us note that the reaction proceeded over the composites without added base, the LDH itself was basic enough to promote the

coupling, although adding more base improved the performance of the catalytic system.

Finally, let us point out that ICP measurement showed no iron ions in the reaction mixture after the repeated runs of each reaction type, *i.e.*, leaching was not a problem even with the Fe(III)-histidinate-CaAl-LDH composite containing some (probably minor portion) of the complexes adsorbed on the outer surface as well.

4. Conclusions

Composite materials containing Fe(III)-amino acid complexes in anionic form as guest and CaAl-LDH as host could be prepared through wet chemical methods (co-precipitation and direct anion exchange). The complex anions were situated mainly among the layers of the LDH, and no leaching was observed during the catalytic reactions. The intercalated complexes have octahedral geometry having water molecules as well as two amino acid anions as bidentate ligands in the coordination sphere. The coordinating atoms/groups could be identified, and it was found that the imidazole and amino nitrogens, the carboxylate oxygen as well as the sulphur atom in the thiolate group were sure coordination sites. The composite materials acted as catalysts in the oxidative transformations of cyclohexene as well as in the Ullmann-type diaryl coupling reaction displaying very good recycling abilities.

Acknowledgment

This work was supported by the National Science Fund of Hungary through grant OTKA NKFI 106234 and grant GINOP-2.3.2-15-2016-00013. The financial help is highly appreciated.

References

- [1] K.M. Koeller, C.H. Wong, *Nature* 409 (2001) 232–240.
- [2] U. Hanefeld, L. Gardossi, E. Magner, *Chem. Soc. Rev.* 38 (2009) 453–468.
- [3] U.T. Bornscheuer, *Angew. Chem. Int. Ed.* 42 (2003) 3336–3337.
- [4] M. Sharma, B. Das, G.V. Karunakar, L. Satyanarayana, K.K. Bania, *J. Phys. Chem. C* 120 (2016) 13563–13573.
- [5] R.S. Weber, P. Gallezot, F. Lefebvre, S.L. Suib, *Mic. Mater.* 1 (1993) 223–227.
- [6] T.J. Pinnavaia, M. Chibwe, V.R.L. Constantino, S.K. Yun, *Appl. Clay Sci.* 10 (1995) 117–129.
- [7] K. Zhu, D. Wang, J. Liu, *Nano Res.* 2 (2009) 1–29.
- [8] Z. Cséndes, Cs. Dudás, G. Varga, É.G. Bajnóczi, S.E. Canton, P. Sipos, I. Pálinkó, *J. Mol. Struc.* 1044 (2013) 39–45.
- [9] B.M. Weckhuysen, A.A. Verberckmoes, L. Fu, R.A. Schoonheydt, *J. Phys. Chem.* 100 (1996) 9456–9461.
- [10] F. Zhang, X. Zhao, C. Feng, B. Li, T. Chen, W. Lu, X. Lei, S. Xu, *ACS Catal.* 1 (2011) 232–237.
- [11] H. Liang, F. Meng, M. Cabán-Acevedo, L. Li, A. Forticaux, L. Xiu, Z. Wang, S. Jin, *Nano Lett.* 15 (2015) 1421–1427.
- [12] T. Yatabe, X. Jin, K. Yamaguchi, N. Mizuno, *Angew. Chem. Int. Ed.* 54 (2015) 13302–13306.

- [13] G. Centi, S. Perathoner, *Mic. Mes. Mater.* 107 (2008) 3–15.
- [14] N. Bette, J. Thielemann, M. Schreiner, F. Mertens, *ChemCatChem* 8 (2016) 1–5.
- [15] Q. Fan, X. Li, Z. Yang, J. Han, S. Xu, F. Zhang, *Chem. Mater.* 28 (2016) 6296–6304.
- [16] K. Yamaguchi, K. Mori, T. Mizugaki, K. Ebitani, K. Kaneda, *J. Org. Chem.* 65 (2000) 6897–6903.
- [17] M. Sipiczki, A.A. Ádám, T. Anitics, Z. Cséndes, G. Peintler, Á. Kukovecz, Z. Kónya, P. Sipos, I. Pálinkó, *Catal. Today* 241 (2015) 231–236.
- [18] O. Kikhtyanin, E. Lesnik, David Kubíčka, *Appl. Catal. A* 525 (2016) 215–225.
- [19] L. Mohapatra, K. Parida, *J. Mater. Chem. A* 4 (2016) 10744–10747.
- [20] S.J. Mills, A.G. Christy, J.M.R. Génin, T. Kameda, F. Colombo, *Miner. Mag.* 76 (2012) 1289–1336.
- [21] C. de Roy, Layered Double Hydroxides, in: V. Rives (Ed.), Nova Science Publishers, Inc., 2001, 2016, pp. 1–39, Ch. 1.
- [22] J. He, M. Wei, B. Li, Y. Kang, D.G. Evans, X. Duan, *Struct. Bond.* 119 (2005) 89–119.
- [23] V. Rives, M.A. Ulibarri, *Coord. Chem. Rev.* 181 (1999) 61–120.
- [24] M. Halma, K.A.D. de Freitas Castro, C. Taviot-Gueho, V. Prevot, C. Forano, F. Wypych, S. Nakagaki, *J. Catal.* 257 (2008) 233–243.
- [25] K.A.D. de Freitas Castro, A. Bail, P.B. Groszewicz, G.S. Machado, W.H. Schreiner, F. Wypych, S. Nakagaki, *Appl. Catal. A* 386 (2010) 51–59.
- [26] X. Wang, G. Wu, X. Liu, C. Zhang, Q. Lin, *Catal. Lett.* 146 (2016) 620–628.
- [27] G. Varga, Á. Kukovecz, Z. Kónya, L. Korecz, Sz. Muráth, Z. Cséndes, G. Peintler, S. Carlson, P. Sipos, I. Pálinkó, *J. Catal.* 335 (2016) 125–134.
- [28] G. Varga, Sz. Ziegenheim, Sz. Muráth, Z. Cséndes, Á. Kukovecz, Z. Kónya, S. Carlson, L. Korecz, E. Varga, P. Puszta, P. Sipos, I. Pálinkó, *J. Mol. Catal. A* 423 (2016) 49–60.
- [29] G.N. George, I.F. Pickering, EXAFSPAK-A Suite of Computer Programs for Analysis of X-ray Absorption Spectra, Stanford Synchrotron Radiation Laboratory, Stanford, CA, 1995, <http://www-ssrl.slac.stanford.edu/exafspak.html> (Accessed May, 2016).
- [30] F. Ullmann, P. Sponagel, *Chem. Ber.* 38 (1905) 2211–2212.
- [31] Q. Wang, D. O'Hare, *Chem. Rev.* 112 (2012) 4124–4155.
- [32] M. Sacerdoti, E. Passaglia, Neues Jahrbuch für Mineralogie, monatshefte, in: Hydrocalumite from Latium, Italy: Its Crystal Structure and Relationship with Related Phases, 1988, pp. 462–475.
- [33] T.E. Westre, P. Kenneppohl, J.G. de Witt, B. Hedman, K.O. Hodgson, E.I. Solomon, *J. Am. Chem. Soc.* 119 (1997) 6297–6314.
- [34] G. Varga, Z. Cséndes, G. Peintler, O. Berkési, P. Sipos, I. Pálinkó, *Spectrochim. Acta A* 122 (2014) 257–259.
- [35] J.-H. In, S.-E. Park, R. Song, W. Nam, *Inorg. Chim. Acta* 343 (2003) 373–376.
- [36] F. Monnier, M. Taillefer, *Angew. Chem. Int. Ed.* 48 (2009) 6954–6971.
- [37] O. Bistri, A. Correa, C. Bolm, *Angew. Chem. Int. Ed.* 47 (2008) 586–588.